

AD-A268 370



PROCEEDINGS REPRINT

SPIE—The International Society for Optical Engineering

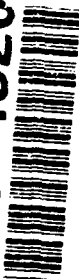
Reprinted from

Optics of the Air-Sea Interface: Theory and Measurement

23-24 July 1992
San Diego, California

DTIC
ELECTE
AUG 19 1993
S A D

93-19204



This document has been approved
for public release and sale; its
distribution is unlimited



Volume 1749

93 8 18 02 4

©1992 by the Society of Photo-Optical Instrumentation Engineers
Box 10, Bellingham, Washington 98227 USA. Telephone 206/676-3290.

REPORT DOCUMENTATION PAGE

Form Approved
OBM No. 0704-0188

Public reporting burden for this collection of information is estimated to average 1 hour per response, including the time for reviewing instructions, searching existing data sources, gathering and maintaining the data needed, and completing and reviewing the collection of information. Send comments regarding this burden or any other aspect of this collection of information, including suggestions for reducing this burden, to Washington Headquarters Services, Directorate for Information Operations and Reports, 1215 Jefferson Davis Highway, Suite 1204, Arlington, VA 22202-4302, and to the Office of Management and Budget, Paperwork Reduction Project (0704-0188), Washington, DC 20503.

1. Agency Use Only (Leave blank).		2. Report Date. July 1992	3. Report Type and Dates Covered. Final - Proceedings	
4. Title and Subtitle. Dependence of Ocean Heating on the Distribution of Spectral Irradiance in the North Atlantic			5. Funding Numbers. <i>Contract</i> <i>Program Element No.</i> 0603741D <i>Project No.</i> 0101 <i>Task No.</i> 100 <i>Accession No.</i> DN259069 <i>Work Unit No.</i> 93522B	
6. Author(s). Robert A. Arnone, Gregory E. Terrie, and Paul J. Martin				
7. Performing Organization Name(s) and Address(es). Naval Research Laboratory Oceanography Division Stennis Space Center, MS 39529-5004			8. Performing Organization Report Number. PR 92:109:321	
9. Sponsoring/Monitoring Agency Name(s) and Address(es). Naval Research Laboratory Advanced Acoustics Program Office Stennis Space Center, MS 39529-5004			10. Sponsoring/Monitoring Agency Report Number. PR 92:109:321	
11. Supplementary Notes. Published in SPIE.				
12a. Distribution/Availability Statement. Approved for public release; distribution is unlimited.			12b. Distribution Code.	
13. Abstract (Maximum 200 words). <p>Subsurface heating rates from visible solar irradiance were computed for the North Atlantic for May 1979 during the period of the spring bloom. The visible spectrum between 400 and 700 nm accounts for a substantial fraction, about 43%, of the total solar irradiance at the sea surface, and comprises most of the solar irradiance that penetrates more than a meter into the sea. The mean monthly spectral diffuse attenuation coefficients and surface solar irradiance were used to compute heating rates at 390, 440, 490, 540, 590, 640, and 690 nm over depth increments of 0-5, 5-10, 10-15, 15-20, and 20-35 m. At low latitudes, in the North Atlantic, significant solar heating occurs at depth as a consequence of high solar irradiance and clear waters. In the northern latitudes the heating is confined near the surface at all wavelengths as a result of high turbidity. Significant spatial variation in the spectral heating rates is observed as a result of chlorophyll and aerosol patchiness.</p>				
14. Subject Terms. Optics, data base, satellite, remote sensing			15. Number of Pages. 10	
			16. Price Code.	
17. Security Classification of Report. Unclassified	18. Security Classification of This Page. Unclassified	19. Security Classification of Abstract. Unclassified	20. Limitation of Abstract. SAR	

Dependence of Ocean Heating on the Distribution of Spectral Irradiance in the North Atlantic

Robert A. Arnone
Gregory E. Terrie
Paul J. Martin

Naval Research Laboratory
Stennis Space Center, MS 39527

ABSTRACT

Subsurface heating rates from visible solar irradiance were computed for the North Atlantic for May 1979 during the period of the spring bloom. The visible spectrum between 400 and 700 nm accounts for a substantial fraction, about 43%, of the total solar irradiance at the sea surface, and comprises most of the solar irradiance that penetrates more than a meter into the sea. The mean monthly spectral diffuse attenuation coefficients and surface solar irradiance were used to compute heating rates at 390, 440, 490, 540, 590, 640, and 690 nm over depth increments of 0-5, 5-10, 10-15, 15-20, and 20-35 m. At low latitudes, in the North Atlantic, significant solar heating occurs at depth as a consequence of high solar irradiance and clear waters. In the northern latitudes the heating is confined near the surface at all wavelengths as a result of high turbidity. Significant spatial variation in the spectral heating rates is observed as a result of chlorophyll and aerosol patchiness.

1. INTRODUCTION

Direct solar heating of the upper ocean significantly affects physical and biological processes. The distribution of heat near the oceans surface is primarily responsible for stabilizing the surface waters, resulting in thermal and biological gradients which are important for understanding the global carbon cycle and its influence on global warming¹. The rate of solar heating of the sea is controlled by the incident irradiance and the optical properties of the water. The variability in these rates is responsible for the diurnal, seasonal, and climatological scales of thermal evolution in the upper ocean². The surface heat process is responsible in the development of the mixed layer. Approximately half the solar irradiance occurs in the infrared portion of the spectrum and most of this is absorbed and converted to heat in the upper few centimeters. The remaining half of the incident solar irradiance occurs in the visible and ultra-violet portion of the spectrum^{3,4}. The flux of solar irradiance that penetrates below the ocean surface is regulated by optical absorption by the water, phytoplankton, and suspended particles. This absorbed irradiance is mostly converted to heat. Numerical models have shown the importance of direct subsurface solar heating in the upper ocean on vertical mixing³. Vertical heating of the water column has a significant impact on its stability. Enhanced erosion of the seasonal thermocline can occur in areas where substantial subsurface heating occurs, as has been shown for the Pacific^{1,3}. The depth dependence of solar heating is dependent on the wavelength of the incident solar irradiance and the spectral diffuse attenuation coefficient of the water^{1,2,4,5}.

In open ocean water, the diffuse attenuation coefficient is controlled by the phytoplankton concentration^{7,8}. Morel⁵ has derived relations between chlorophyll concentration and the diffuse attenuation coefficient in the visible portion of the solar spectrum from in situ measurements. The spatial variability of the phytoplankton has been shown to be patchy, and the temporal distribution of the phytoplankton has been shown to be highly variable based on satellite ocean color observations^{9,10}. The solar irradiance distribution is also highly variable. This variability is primarily a consequence of variations in cloudiness and aerosol concentrations⁶. The patchiness of both solar irradiance and phytoplankton, causes spatial variations in solar heating.

DTIC QUALITY INSPECTED 3

A-11 20

The objective of this effort is to define the visible irradiance incident at the sea surface and how it is absorbed within the surface waters of the North Atlantic. This paper will define the contribution to heating of the water column for various visible wavelengths resulting from the vertical spectral distribution of irradiance. The North Atlantic in May, 1979 was selected for analysis because of the elevated phytoplankton concentration associated with the spring bloom. High solar irradiance is also observed at this time of year in the North Atlantic.

The general form of the equation for the solar heating rate of the upper ocean is expressed as:

$$\frac{dT}{dt} = \frac{\overline{K_d} \overline{E_{0\lambda}} e^{-\overline{K_d} z}}{\rho C_p}$$

where $K_{d\lambda}$ is the downward diffuse attenuation coefficient and $E_{0\lambda}$ is the downward solar irradiance at the sea surface. Both of these parameters are dependent on wavelength. ρ is the water density, C_p is the heat capacity of water, and z is the water depth.

The diffuse attenuation coefficient that defines the rate of decay of irradiance in the water column is dependent on the vertical distribution of chlorophyll in the open ocean^{5,11}. Our computations assume the chlorophyll concentrations which are observed from satellite ocean color are constant within the upper 35 m. Morel⁵ defined the spectral dependence of $K_{d\lambda}$ based on chlorophyll as:

$$K_d(\lambda) = K_w(\lambda) + \chi_c(\lambda) C^\epsilon(\lambda)$$

where K_w , χ , and ϵ are constants. His results indicate that in water of low chlorophyll concentration the minimum $K_{d\lambda}$ occurs at about 490 nm and that, as the chlorophyll concentration increases, the minimum $K_{d\lambda}$ shifts to about 580 nm (Figure 1).

The spectral visible solar irradiance at the sea surface; $E_{0\lambda}$; is controlled by the extraterrestrial solar spectrum, and the spectral transmittance by the atmosphere, which is primarily governed by the Rayleigh scattering in the atmosphere and the ozone distribution^{6,12}. The magnitude of the incident solar irradiance also depends on time of year, time of day, and latitude.

By coupling the spectral irradiance at the sea surface ($E_{0\lambda}$), and the corresponding spectral diffuse attenuation coefficient of the water column $K_{d\lambda}$, the downward irradiance at any depth $E_{d\lambda}$ can be computed using Beers law. The heating rate can then be computed assuming that within the visible domain the absorbed radiance at a depth is essentially totally converted to heat⁵. Heat associated with photosynthetic storage processes is very small (<2%) and has been neglected¹.

2. METHODS

The Coastal Zone Color Scanner (CZCS) global processing data set was used to obtain a monthly composite of the diffuse attenuation coefficient at 490 nm for May 1979^{9,10}. The monthly K_{d490} optical properties of the

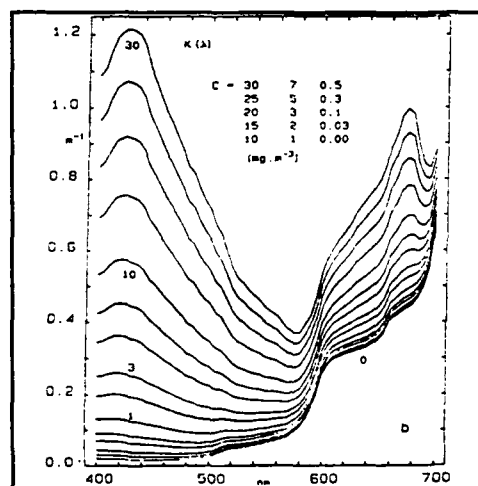


Figure 1. Dependence of $K_{d\lambda}$ on chlorophyll concentration from Morel (1988)⁵.

North Atlantic were obtained from the water leaving radiance at 443 and 550 nm from CZCS ⁷ (Figure 2a). The mean K_{d490} for approximately 20 km squares (at the equator) were computed from all cloud free CZCS data during May 1979. There are several central Atlantic areas where no CZCS data were obtained. The North Atlantic illustrates high attenuation coefficients associated with the spring bloom and the North Sea. The southern and central areas of the Sargasso Sea indicate very clear water, i.e., low K_d values. Notice the patchiness of the optical properties especially in high K_d areas such as coastal and upwelling regions (African coast). The mean K_{d490} monthly data were converted to K_{d390} , K_{d440} , K_{d540} , K_{d590} , K_{d640} , and K_{d690} using the relationships of Austin and Petzold¹³. These visible wavelengths were used to represent heating rates in the visible spectrum.

The incident solar spectral irradiance was computed for May 1979 for the North Atlantic using an extension of Bird's model^{6,12} (figure 2b). This model was used to compute the hourly incident spectral irradiance at seven visible wavelengths (defined above) using (1) the aerosol concentration from La670 of CZCS, (2) the ozone concentration from the Total Ozone Mapping Spectrometer, and (3) cloud cover from the Real Time Nephelanalysis (RTNEPH) Air Force 3-hourly observations. These data bases from May 1979 were used to compute the monthly average solar irradiance at locations coincident with the monthly composite diffuse attenuation coefficient. The spectral dependence of the solar irradiance model is described in Terrie and Arnone ⁶ in this issue. The importance of aerosols, in addition to clouds, is emphasized for certain locations in the North Atlantic (e.g., the African Sahara coast). The irradiance computed at the sea surface is in units of $W/m^2/nm$ and the values obtained compare with other models¹⁴. Figure 2b illustrates elevated irradiance at 490 nm at 20° N, just west of the African coast. A general decrease is observed to the north. A band of decreasing solar irradiance is observed along the Intertropical Convergence Zone because of high cloud cover. Similarly, notice the variability in the irradiance distribution at scales less than 100 km.

3. RESULTS

The average monthly irradiance was computed at 0, 5, 10, 15, 20, and 35 m depth for seven wavelengths (defined above). Figure 3 shows the monthly mean irradiance field at 490 nm at depths of 5 and 35 m. At 5 m the 490 nm wavelength has a similar distribution to the surface irradiance, especially in the clear waters of the Sargasso Sea. In the more turbid areas, such as the North Sea, the irradiance field is strongly absorbed and the distribution appears similar to that of the K_{d490} distribution. Large patches of phytoplankton located south of Greenland have a significant affect on the irradiance field at 5 m. Very high irradiance levels are observed as a "hot" area at 20° N in the central North Atlantic. This area has high surface irradiance and low water attenuation. Similar areas of high incident irradiance and low attenuation water have been observed in the Pacific. In the northern latitudes, high K_d values are observed with decreased solar irradiance. The subsurface irradiance is rapidly attenuated in the surface waters and closely resembles the water attenuation distribution.

The 35-m irradiance field at 490 nm is very different from the surface distribution. The northern latitudes indicate a substantial reduction in the irradiance distribution as a consequence of reduced irradiance and absorption by elevated chlorophyll concentrations. The turbid North Sea waters have little irradiance penetrating to 35 m. The clear waters at 20° N again show the "hot" area suggesting oligotrophic conditions. Near the US east coast the 35-m irradiance field shows the mesoscale features associated with the Gulf Stream. The 35-m field distribution closely resembles the patterns of the K_{d490} data.

Comparisons of spectral irradiance at 10-m depth at 490 nm with 440, 540 and 590 nm are shown in scattergrams for the entire North Atlantic (figure 4). The histograms for the entire North Atlantic are also shown for each scattergram. The 490, 540, and 590 histograms show a unimodal distribution centered at 0.3, 0.25, and 0.05 $W/m^2/nm$ from the "hot" area at 20° N. The histogram of the 440 nm distribution is bi-modal. Note that the higher irradiance distributions are associated with clear waters and/or low latitudes, and that lower irradiance's

represent coastal, high K_d values or high latitude waters. The 440 - 490 comparison shows that clear, high irradiance areas have a nearly covarying (1:1) irradiance relationship, whereas at low irradiance levels (high K_d waters) the 440 irradiance is strongly absorbed and is lower than 490 (0.5:1). The 540 to 490 comparison shows a reverse relationship with low irradiance (higher K_d waters) having slightly higher 540 irradiance than 490 (approximately a 1.2:1). Conversely, similarly for high irradiance (low K_d waters), the 540 irradiance is lower than the 490. In turbid water increased transmittance of light shifts to the higher wavelengths; 540 nm and is responsible for the increase in 540 irradiance over 490. At 590 nm the irradiance is confined to the surface layers. The 490 - 590 irradiance comparison for the entire North Atlantic indicates very low irradiance levels at 10 m and a monotonic relationship with the 490 irradiance.

The average heating rate in the upper 10 m was computed from the subsurface irradiance field. The average heating rate (deg C/day/nm) at 490 and 590 nm is shown in Figure 5. The 490 nm heating rates (figure 5) are lower in the tropical Atlantic even though the irradiance levels are shown to be higher (figure 2b). The low K_d of these waters results in a substantial amount of solar irradiance penetrating below the upper 10 m. In northern latitudes, the heating rate at 490 nm is higher, especially in the high K_d waters of the North Sea. Although the incident irradiance generally is lower in the north, note that the heating rates in the upper 10 m are substantially higher than at the lower latitudes. The 590 nm heating rate (figure 5b) is high throughout the North Atlantic (see histogram Figure 4) showing little variation. The upper 10 m absorbs most of the 590 nm irradiance. The small scale variability that is observed in the figure is related to incident surface irradiance and not to the attenuation coefficient of the water.

Spectral heating rates were computed for the North Atlantic for depth increments of 0-5, 5-10, 10-15, 15-20, and 20-35 m (Figure 6). The mean heating rate in the upper 5 m is greatest at 640 nm because of the combination of high incident solar irradiance at the sea surface and high attenuation in the water (Figure 1) at this wavelength. At wavelengths above 640 nm the heating rate in the upper 5 m is reduced because of lower solar irradiance. At wavelengths below 640, the heating rate is reduced because of the lower attenuation and the resulting increased penetration of irradiance below 5 m. At the deep depths, the maximum heating rate shifts to 440 - 490 nm because of high solar irradiance and low attenuation in the water within this spectral range. At the low to moderate chlorophyll concentrations typical of most of the North Atlantic, the minimum attenuation of solar irradiance occurs at 450 - 500 nm (Figure 1). At wavelengths below 390 nm, the amount of available incident solar irradiance decreases significantly in addition to the penetration depth of irradiance.

4. SUMMARY

This effort represents a convolution of the spectral distribution of solar irradiance and the spectral attenuation of ocean waters. The spectral irradiance at different water depths for the North Atlantic during May 1979 was calculated using satellite derived solar irradiance and water diffuse attenuation coefficient (K_{d490}). These monthly climatologies represent synoptic characterization of the North Atlantic during the spring bloom when chlorophyll concentration are high and the water diffuse attenuation coefficient is elevated. The incident solar spectral irradiance and the water's diffuse attenuation coefficient were used to compute the irradiance at 5 and 35 m. The irradiance distributions at 5 m was similar to the incident solar irradiance especially in the tropical Atlantic where the water K_{d1} was small. A elevated irradiance "hot" area was observed at 20° N where clear water permitted significant irradiance penetration to depth (35 m). North latitudes had reduced incident irradiance and elevated attenuation from the high chlorophyll blooms. Minimal irradiance was observed at depth at these latitudes. Spectral comparisons of the 490 nm irradiance and 440 and 590 nm distribution at 10 m were illustrated in scattergrams and histograms. The 440 and 490 nm irradiance fields are similar in low K_d waters which comprise the majority of the North Atlantic. Differences occur in the higher K_d waters (coastal) where the irradiance distribution are less penetrating. With the assumption that the subsurface irradiance is totally absorbed and converted to heat, the spectral heating rates were computed for five depth increments (0-5, 5-10, 10-15, 15-20,

and 20-35 m) at seven wavelengths (390, 440, 490, 540, 590, 640, and 690 nm). The spatial variability of the bio-optical properties coupled with the spatial variability of the surface solar irradiance distribution, results in a wide variability in the heating rates in the northern and tropical North Atlantic.

The general distributions observed in this analysis show that major latitudinal differences occur in heating rates in addition to small-scale variability. The low K_d , high irradiance waters observed at 20° N show that substantial solar heating occurs at depth in these regions. Contrastingly, the northerly waters with high K_d , show that very little heating occurs at depth.

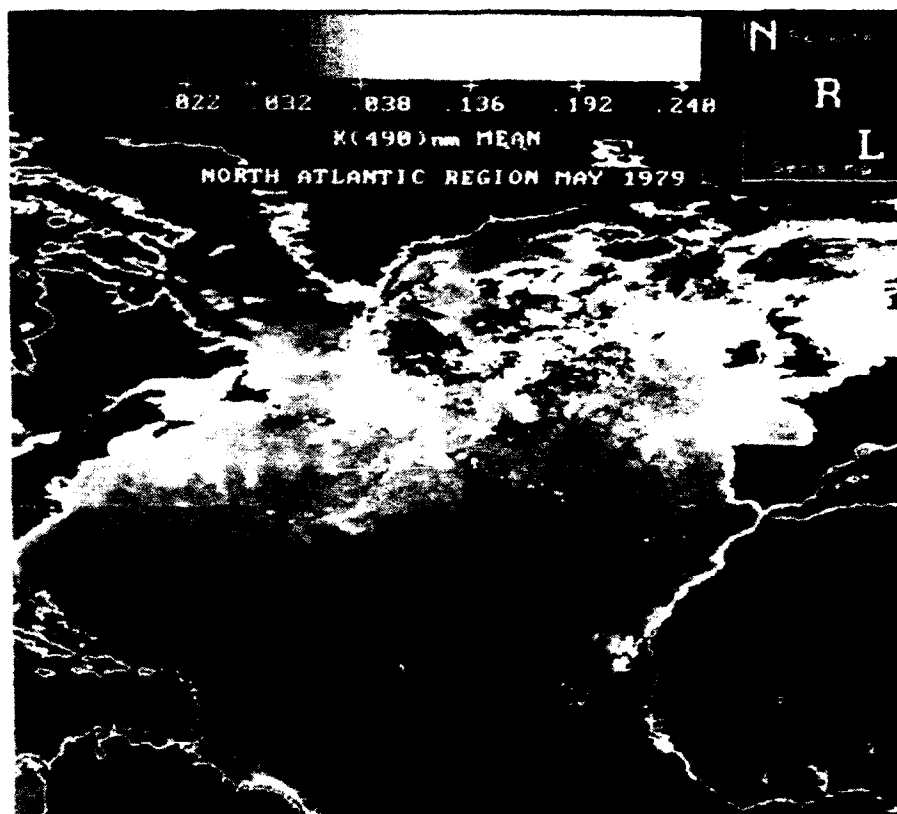
Additional efforts are required to understand the temporal variability of spectral heating rates. Improved satellite sensors will provide new looks at these problems to help understand the coupling of air-sea interactions and their affects on subsurface thermodynamics.

5. ACKNOWLEDGMENTS

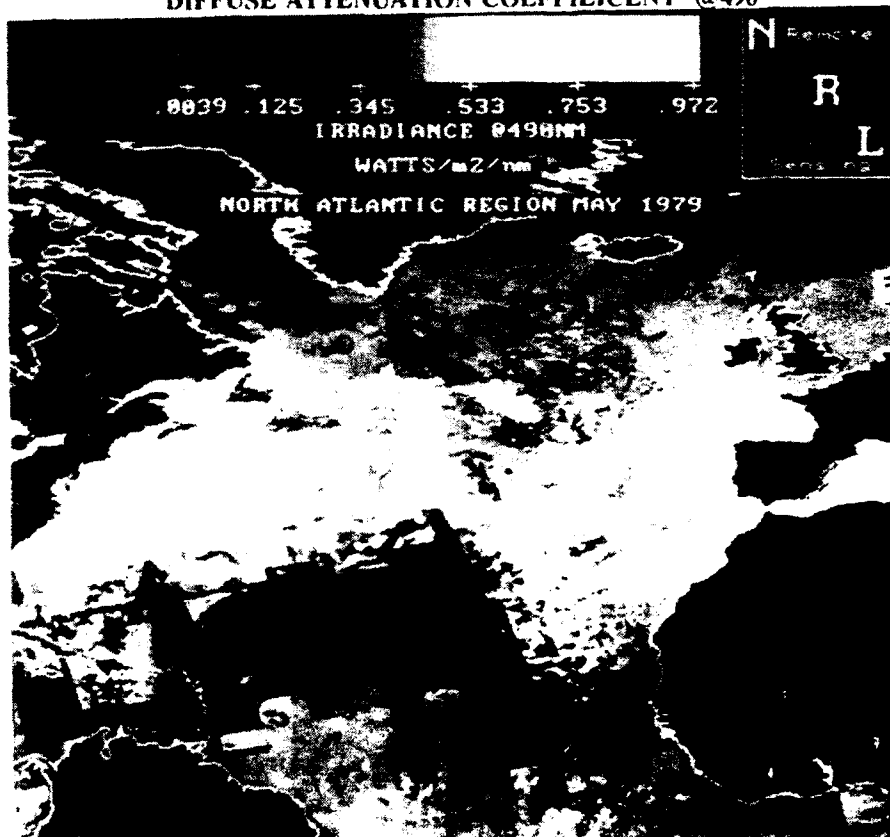
This effort was support by the Air Defense Initiative (PE 0603741D) program manager Gerald Morris and the Oceanographer of the Navy OP096 (PE 0603704N) program manager K. Ferer. Appreciation is extended to S. Oriol for processing support. Thanks is extended to C. McClain and G Fu for providing PC SeaPak software support in which all processing was performed. Gratitude is extended to G. Feldman for the CZCS data set. Thanks is extended to A. Weidemann for beneficial discussions.

6. REFERENCES

1. Lewis, M.R., M.E. Carr, G.Feldman, C.McClain and W. Esaias, "Influence of Penetrating Solar Radiation on the Heat Budget of the Equatorial Pacific Ocean." *Nature* 347:543-545, 1990.
2. Woods, J.D., W. Barkmann and A. Horch, "Solar Heating of the Oceans- Diurnal, Seasonal and Meridional Variation." *Quart. J. Roy. Met. Soc.* 110:663-668, 1984.
3. Martin, P., "Simulation of the Mixed Layer at OWS November and Papa with Several Models." *J. Geophy. Res.* 90:903-916, 1985.
4. Ivanoff, A. " Oceanic Absorption of Solar Energy." Kraus (ed) *Modeling and Prediction of the Upper Layers of the Ocean* Pergamon Press, New York p 47-71, 1977.
5. Morel, A., "Optical Modeling of the Upper Ocean in Relation to its Biogenous Matter Content (Case I Waters)." *J. Geophy. Res* 93: 10,749-10,768, 1988.
6. Terrie, G. and R.A. Arnone, "Spectral and Spatial Variability of Solar Irradiance in the North Atlantic." *SPIE Proceedings, Optics of the Air-Sea Interface: Theory and Measurement*, Vol 1749, this issue, 1992.
7. Austin, R.W. and T.J. Petzold, "The Remote Sensing of the Diffuse Attenuation Coefficient of Sea Water using the Coastal Zone Color Scanner." In J.F.R. Gower (ed) *Oceanography from Space*, Plenum, New York, pp 239-256, 1981.
8. Lewis, M.R., J. Cullen, and T. Platt, "Phytoplankton and Thermal Structure in the Upper Ocean: Consequences of Nonuniformity in Chlorophyll Profile." *J. Geophys. Res.* 88:256-2570, 1983.
9. Feldman, G., W. G. Esaias, C. R. McClain, R. Evans, R. Brown, and J. Edrod, "Ocean Color: Availability of the Global Data Set." *EOS Tran. AGU* 70:23,643, 1989.
10. Arnone, R.A., R.A.Oriol, G. Terrie and L. Estep, "Ocean Optical Database." Naval Oceanographic and Atmospheric Research Laboratory, Technical Note 254, May, 1992.
11. Sathyendranath, S., and T. Platt, "Remote Sensing of Ocean Chlorophyll: Consequence of Nonuniform Pigment Profile." *Ap. Opt.* 28:490-495, 1989.
12. Bird, R. E., "A Simple Solar Spectral Model for Direct-Normal and Diffuse Horizontal Irradiance." *Solar Energy* 32:461-471, 1984.
13. Austin, R.A. and T.J. Petzold, "Spectral Dependence of the Diffuse Attenuation Coefficient of Light in Ocean Waters.", *Opt. Eng.*, 25,471-479, 1986.



DIFFUSE ATTENUATION COEFFICIENT @490



SOLAR IRRADIANCE AT THE SEA SURFACE @490

Figure 2 a: Diffuse Attenuation Coefficient (490) for May 1979

b: Solar Irradiance (490) at the Sea Surface for May 1979

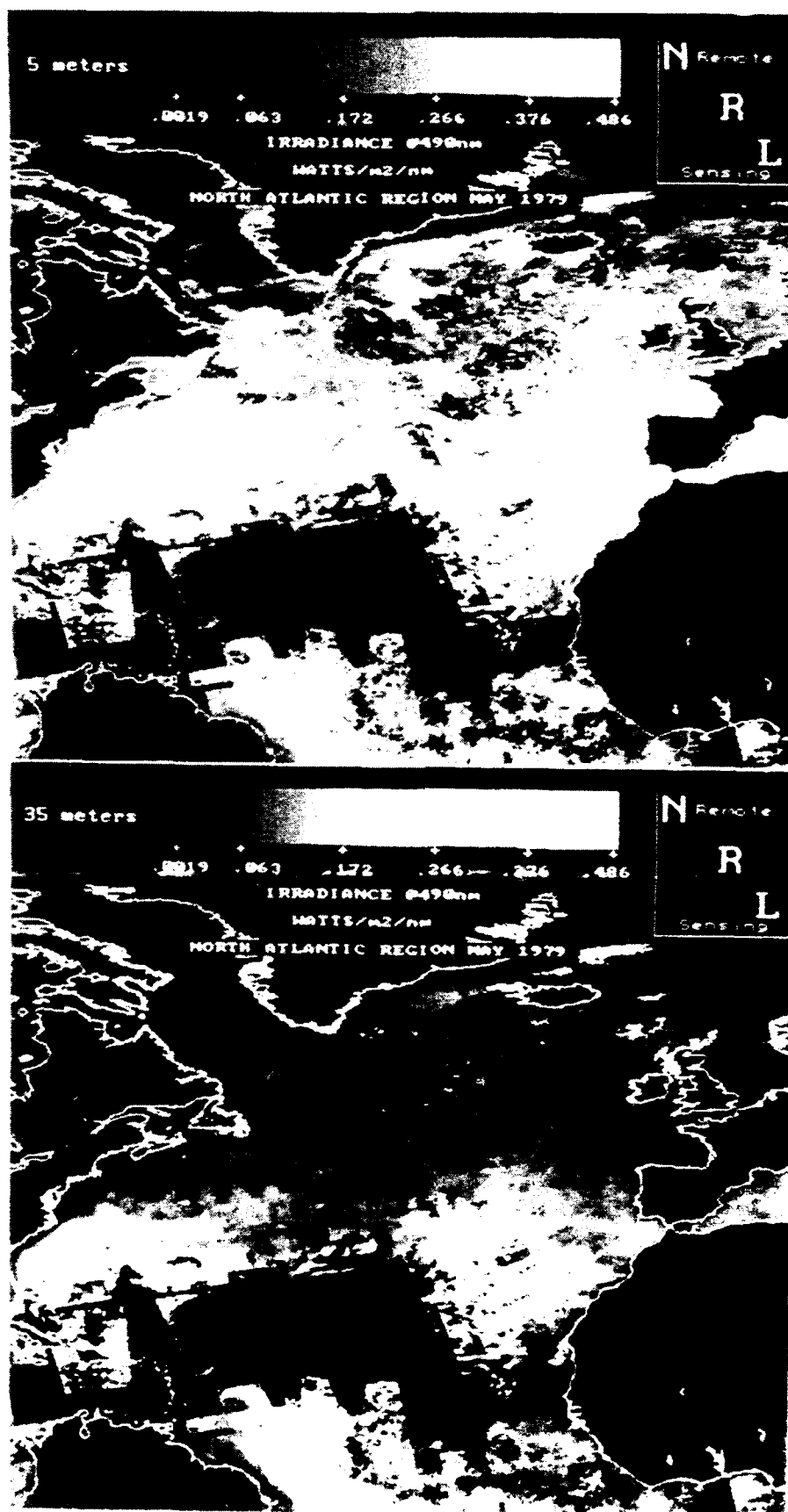


Figure 3. The 490 nm irradiance distribution at 5 and 35 meters depth.

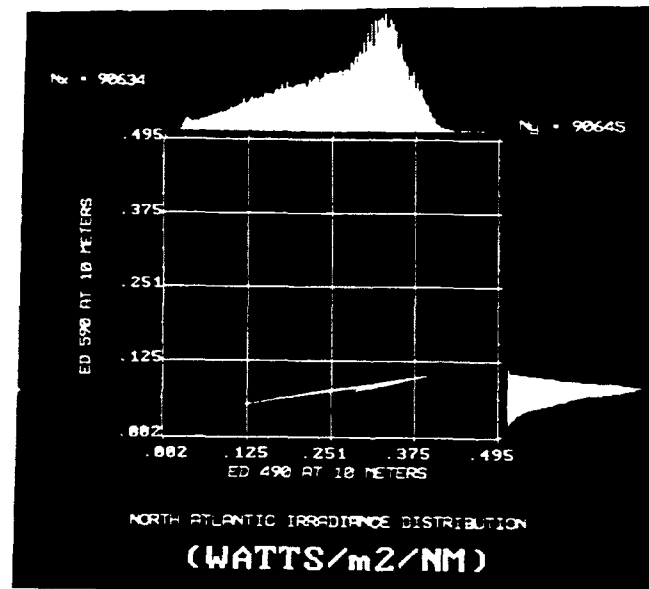
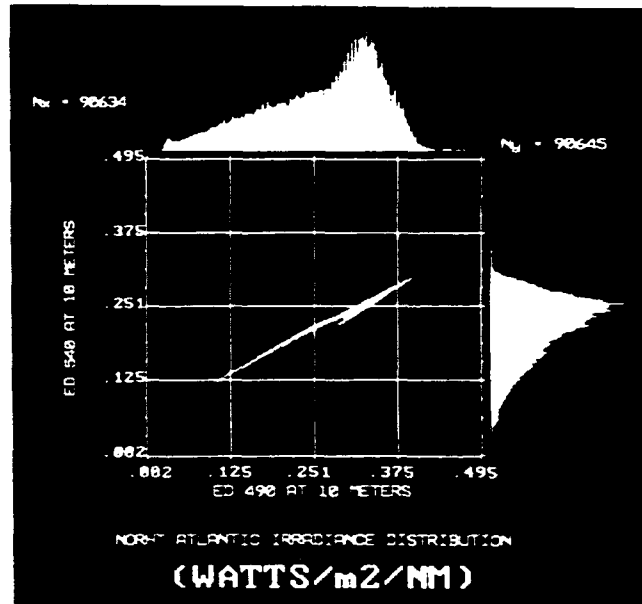
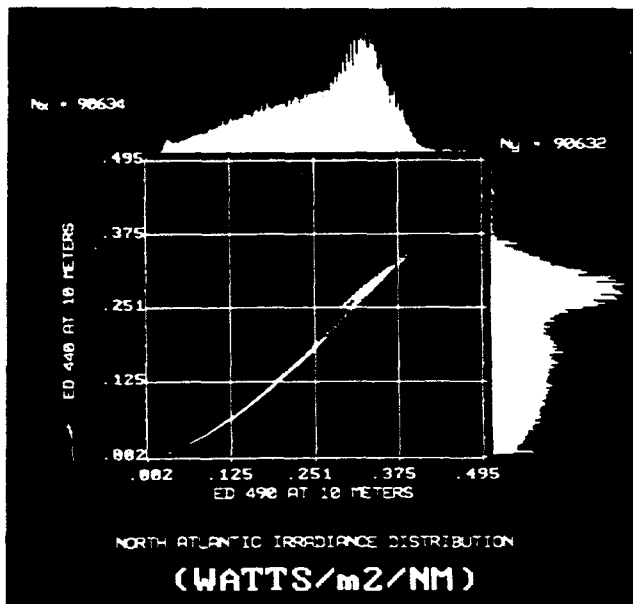


Figure 4. Comparison of the spectral irradiance at 10 meter depth for the entire North Atlantic is shown in these scattergrams. Coincident 440, 540 and 590 nm irradiance values (y-axis) are compared against the 490 nm irradiance values (x-axis) for the entire image field. The histogram of the North Atlantic irradiance is shown in on the side of the axis. The relationship shown by these curves is related to the spectral attenuation of water column. The scatter in the relationship is related to differences in the solar spectral irradiance distribution. The peak of the irradiance observed in the histograms is associated with very clear waters in the central south Atlantic east of Africa where a "hot" spot occurs.

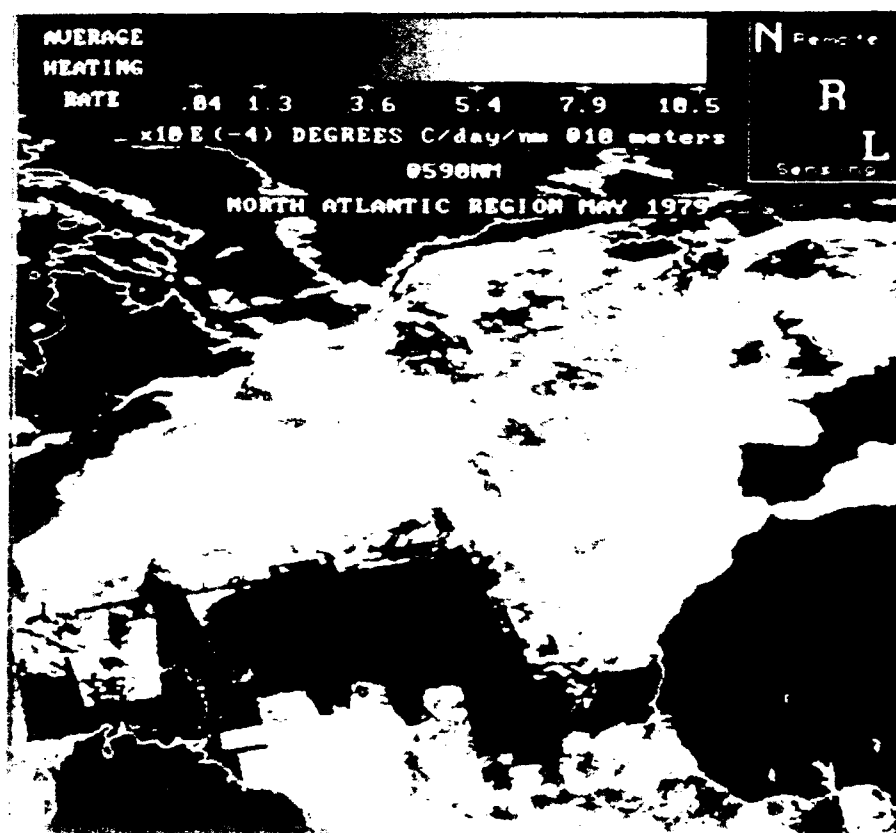


Figure 5. The average heating rates in the upper 10 meters at 490 and 590 nm for May 1979.

Spectral Heating in North Atlantic

Mean heating Rate within Depth Increment

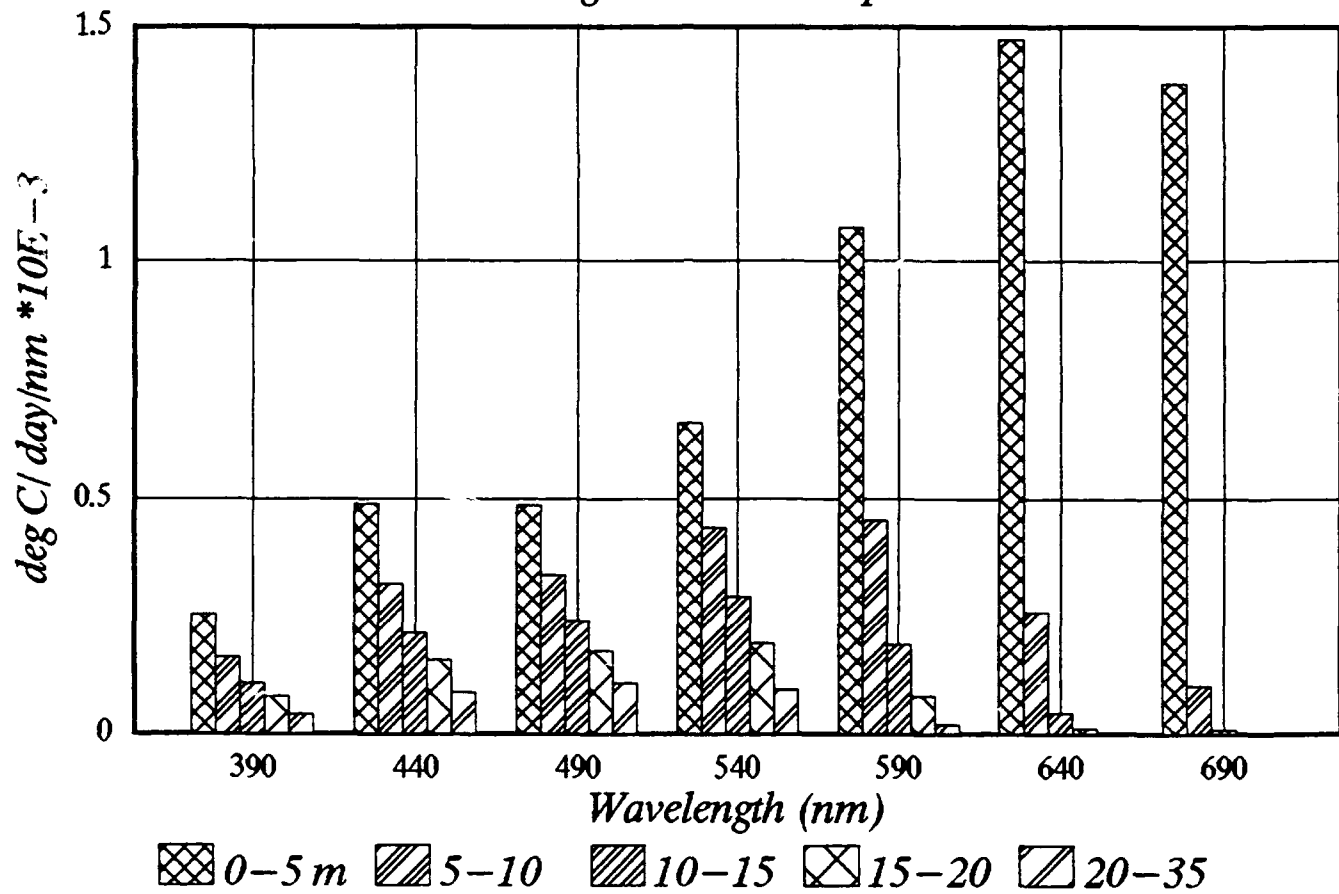


Figure 6: The Mean Spectral Heating Rate in the North Atlantic